

Cutaneous immunosurveillance by self-renewing dermal $\gamma\delta$ T cells

Nital Sumaria,¹ Ben Roediger,¹ Lai Guan Ng,⁵ Jim Qin,¹ Rachel Pinto,² Lois L. Cavanagh,¹ Elena Shklovskaya,¹ Barbara Fazekas de St. Groth,^{1,3} James A. Triccas,² and Wolfgang Weninger^{1,3,4}

¹The Centenary Institute, Newtown, NSW 2042, Australia

²Microbial Pathogenesis and Immunity Group, Discipline of Infectious Diseases and Immunology, ³Discipline of Dermatology, University of Sydney, Camperdown 2006, NSW, Australia

⁴Department of Dermatology, Royal Prince Alfred Hospital, Camperdown 2050, NSW, Australia

⁵Singapore Immunology Network (SIgN), Agency for Science, Technology and Research (A*STAR), Biopolis, Singapore 138648

The presence of $\gamma\delta$ T cell receptor (TCR)–expressing cells in the epidermis of mice, termed dendritic epidermal T cells (DETCs), is well established. Because of their strict epidermal localization, it is likely that DETCs primarily respond to epithelial stress, such as infections or the presence of transformed cells, whereas they may not participate directly in dermal immune responses. In this study, we describe a prominent population of resident dermal $\gamma\delta$ T cells, which differ from DETCs in TCR usage, phenotype, and migratory behavior. Dermal $\gamma\delta$ T cells are radioresistant, cycle in situ, and are partially dependent on interleukin (IL)–7, but not IL–15, for their development and survival. During mycobacterial infection, dermal $\gamma\delta$ T cells are the predominant dermal cells that produce IL–17. Absence of dermal $\gamma\delta$ T cells is associated with decreased expansion in skin draining lymph nodes of CD4⁺ T cells specific for an immunodominant *Mycobacterium tuberculosis* epitope. Decreased CD4⁺ T cell expansion is related to a reduction in neutrophil recruitment to the skin and decreased BCG shuttling to draining lymph nodes. Thus, dermal $\gamma\delta$ T cells are an important part of the resident cutaneous immunosurveillance program. Our data demonstrate functional specialization of T cells in distinct microcompartments of the skin.

CORRESPONDENCE

Wolfgang Weninger:
w.weninger@centenary.org.au

Abbreviations used: BCG, Bacille Calmette–Guérin; DDC, dermal DC; DETC, dendritic epidermal T cell; LC, Langerhans cell.

Peripheral organs, such as the skin, gastrointestinal tract, and lungs, are barriers against invading microorganisms. The immune system deploys sentinels, including DCs, macrophages, and T lymphocytes, to counteract pathogen invasion upon barrier breach within these organs. Some of these cell lineages, in particular DCs, show strict microcompartmental segregation. Thus, the epidermis harbors Langerhans cells (LCs), whereas the dermis is home to at least three subpopulations of dermal DCs (DDCs). Recently, distinct functions have been ascribed to epidermal and DDC subsets (Heath and Carbone, 2009; Nestle et al., 2009; Ueno et al., 2010), indicating adaptation of these cells to their specific anatomical niches. In mouse epidermis, a prominent population of $\gamma\delta$ TCR–expressing T cells, known as dendritic epidermal T cells (DETCs), can be found. Whether the dermis also contains a discrete population of $\gamma\delta$ T cells and, if so, what role these cells may play in immune defense has been investigated only perfunctorily.

Many studies have documented a remarkable enrichment of $\gamma\delta$ T lymphocytes within the epithelia of peripheral organs; they otherwise represent only a minority of the T cell pool in secondary lymphoid organs. Curiously, these epithelial T cells often display restricted TCR repertoires. Thus, DETCs bear the canonical V γ 5/V δ 1 TCR (TCR nomenclature; Heilig and Tonegawa, 1986; Asarnow et al., 1988; Havran et al., 1989). Similarly, the lungs, gastrointestinal tract, and genitourinary tract are populated with distinctive subsets of $\gamma\delta$ T cells bearing tissue-specific TCRs with limited or invariant diversity (Carding and Egan, 2002; Xiong and Raulet, 2007; Bonneville et al., 2010). This expression of specific TCRs points toward functional specialization of these cells

© 2011 Sumaria et al. This article is distributed under the terms of an Attribution–Noncommercial–Share Alike–No Mirror Sites license for the first six months after the publication date (see <http://www.rupress.org/terms>). After six months it is available under a Creative Commons License (Attribution–Noncommercial–Share Alike 3.0 Unported license, as described at <http://creativecommons.org/licenses/by-nc-sa/3.0/>).

and suggests that they may react to a limited spectrum of antigens. It is generally believed that $\gamma\delta$ T cells respond to self-antigens induced on stressed or infected cells or to microbial antigens mediated by signals delivered via the TCR, Toll-like receptors, and/or NKG2D (Havran et al., 1991; Nitahara et al., 2006). However, unlike their $\alpha\beta$ T cell counterparts, $\gamma\delta$ T cells recognize antigens without the requirement for antigen processing and presentation by classical MHC molecules (Tanaka et al., 1995). Upon stimulation, $\gamma\delta$ T cells produce a variety of mediators and cytokines and are capable of cell-mediated cytotoxicity. Recently, it has been proposed that there exist two functionally distinct subsets of $\gamma\delta$ T cells within lymphoid organs: an antigen-naïve subset that rapidly secretes IL-17 upon activation and antigen-experienced cells that primarily produce IFN- γ (Jensen et al., 2008; Ribot et al., 2009).

DETCs are the first T cells to develop in the fetal thymus and seed the epidermis during development in a temporally highly regulated manner (Havran and Allison, 1988). Furthermore, DETCs in adult mice are restricted to the epidermis and are absent from systemic circulation, lymphoid organs, and other epithelial sites. In the mouse, DETCs have been implicated in both epidermal homeostasis and repair (Boismenu and Havran, 1994; Jameson et al., 2002; Sharp et al., 2005). In addition to maintaining epithelial integrity and barrier function, DETCs may protect against the development of cutaneous malignancies and regulate the inflammatory response (Girardi et al., 2001, 2002, 2003).

Based on their localization to the epidermis and their restricted TCR expression, it is debatable whether DETCs actively participate in dermal immunosurveillance. Given the nonredundant role of $\gamma\delta$ T lymphocytes in the immune response against pathogens, we wondered whether the dermis also contains resident $\gamma\delta$ T cells. In this study, we have identified a robust population of dermal $\gamma\delta$ T cells. These cells expressed a mixed panel of TCRs and differed in their survival requirements and functional properties from their epidermal counterparts. Furthermore, dermal $\gamma\delta$ T cells regulated antigen-specific CD4⁺ T cell responses after dermal mycobacterial infection. Together, these results define a population of $\gamma\delta$ T cells in the dermis of mice that participates in cutaneous immune responses. Our results further highlight the compartmental specialization of cutaneous T cell populations that exhibit separable functions in the immune surveillance program.

RESULTS

Mouse dermis harbors a prominent population of $\gamma\delta$ T cells

To determine the presence of $\gamma\delta$ T cells within the individual compartments of the skin, we prepared single-cell suspensions from dermal and epidermal sheets of C57BL/6 mouse ears. Consistent with previous studies (Hayday, 2000; Bonneville et al., 2010), we found that 100% of epidermal CD3⁺ leukocytes represented $\gamma\delta$ T cells, of which $\sim 98\%$ were V γ 5⁺ (Fig. 1, A and B). Strikingly, we identified an abundant population of $\gamma\delta$ T cells in the dermis. $\gamma\delta$ T cells constituted $54.1 \pm 5.4\%$ of dermal T cells (Fig. 1, A and B), of which 80% were V γ 5⁺ (Fig. 1, A and B) and were therefore distinct from their epidermal counterparts. The V γ 5⁺ dermal $\gamma\delta$ T cell population may represent either epidermal contaminants, e.g., from residual hair follicles in the dermal sheet preparation, or bona fide dermal residents. Further analyses on TCR usage showed that $\sim 30\%$ of dermal $\gamma\delta$ T cells expressed V γ 4 TCR (Fig. 1 C), demonstrating that, unlike DETCs, dermal $\gamma\delta$ T cells are a heterogeneous population.

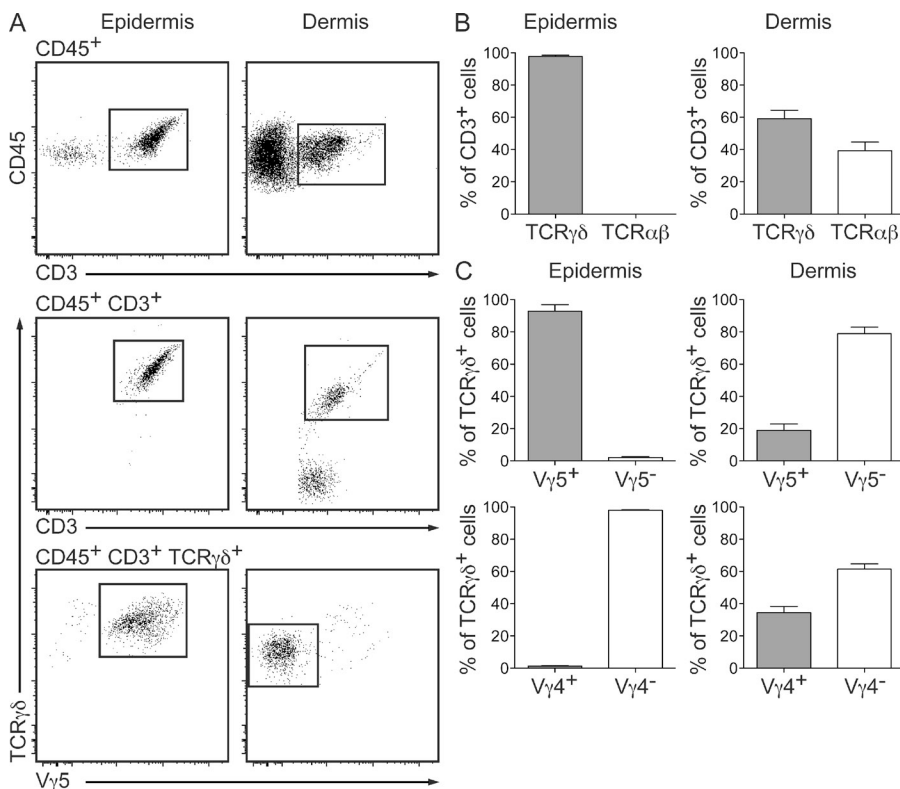


Figure 1. The mouse dermis harbors a population of $\gamma\delta$ T cells. (A) Flow cytometry profiles of epidermal and dermal $\gamma\delta$ T cells from ear skin of WT mice ($n \geq 9$ /group). Cells were gated on CD45⁺ (top), CD45⁺CD3⁺ (middle), or CD45⁺CD3⁺TCR $\gamma\delta$ ⁺ (bottom). (B) Percentage of $\alpha\beta$ T cells and $\gamma\delta$ T cells within dermal and epidermal CD3⁺ cells of ear skin in WT mice ($n = 9$). (C) TCR $\gamma\delta$ usage of epidermal and dermal $\gamma\delta$ T cells from WT mice ($n = 9$). Results are expressed as a frequency of TCR $\gamma\delta$ ⁺ T cells. Data are representative of at least two independent experiments. Data are presented as mean \pm SEM.

We next undertook a comprehensive phenotypic characterization of DETCs and dermal $\gamma\delta$ T cells in steady-state skin (Fig. 2). Dermal $\alpha\beta$ T cells and splenic $\gamma\delta$ T cells were included in the analyses for comparison. Dermal $\alpha\beta$ and $\gamma\delta$ T cells expressed low levels of CD25, whereas DETCs and splenic $\gamma\delta$ T cells were CD25⁺. Although all epidermal and splenic $\gamma\delta$ T cells expressed high levels of CD43, the expression of this marker on dermal $\gamma\delta$ T cells was bimodal. All cutaneous T cells were CD44⁺, whereas splenic $\gamma\delta$ T cells had bimodal expression of CD44. Remarkably, all cutaneous T cells were CD69⁺, suggesting a preactivated state. Splenic $\gamma\delta$ T cells were CD69⁺. In addition, cutaneous, but not splenic, T cells expressed CD103 (α_E integrin), a ligand for E-cadherin. CD127 (IL-7R α) was expressed by all skin T cell subsets and, to a lesser extent, by splenic $\gamma\delta$ T cells.

Collectively, these results indicate that the dermis harbors a population of $\gamma\delta$ T cells that represents >50% of CD3⁺ T cells and differs in TCR usage and phenotype from both DETCs and systemic $\gamma\delta$ T cells.

Dermal $\gamma\delta$ T cells are largely radioresistant and proliferate locally in the skin

DETCs have previously been shown to be radioresistant (Honjo et al., 1990) and are not replenished from the bone marrow in adult mice. To assess the radiosensitivity of dermal $\gamma\delta$ T cells, we generated bone marrow chimeras by transplanting CD45.1⁺ bone marrow into lethally irradiated congenic CD45.2⁺ C57BL/6 mice. As expected, 12 wk after transplantation, 100% of V γ 5⁺ DETCs remained host-derived

(CD45.2⁺; Fig. 3 A). Strikingly, $90.9 \pm 2.4\%$ of dermal $\gamma\delta$ T cells also remained of host origin, whereas $\sim 10\%$ of dermal V γ 5⁺ $\gamma\delta$ T cells were donor-derived (Fig. 3 A). In stark contrast, the vast majority of $\gamma\delta$ T cells, including those in the blood, secondary lymphoid organs, and gastrointestinal tract of chimeric mice had been replaced with donor-derived cells (Fig. 3 A). As in other organs, dermal $\alpha\beta$ T cells were predominantly of donor origin (Fig. 3 A). These results suggested that, contrary to $\gamma\delta$ T cells in other organs and dermal $\alpha\beta$ T cells, dermal $\gamma\delta$ T cells are largely maintained independent of circulating precursors.

We therefore hypothesized that dermal $\gamma\delta$ T cells undergo homeostatic proliferation within the dermis. To test this, we examined BrdU incorporation of skin $\alpha\beta$ and $\gamma\delta$ T cells. After 6 d of supplementing the drinking water of C57BL/6 mice, we found that 2% of DETCs had incorporated BrdU, whereas $\sim 6\%$ of both $\gamma\delta$ T cells and $\alpha\beta$ T cells were BrdU⁺ (Fig. 3 B). Because BrdU incorporation could have occurred within bone marrow or thymic precursors before their development into $\gamma\delta$ T cells, we also analyzed BrdU uptake by dermal $\gamma\delta$ T cells in bone marrow chimeras 19 mo after reconstitution. At this point, $\sim 80\%$ of dermal $\gamma\delta$ T cells were still host-derived, whereas $\alpha\beta$ T cells had been almost completely replaced by donor bone marrow (Fig. 3 C). 6 d after BrdU administration, $\sim 4\%$ of both host- and donor-derived dermal $\gamma\delta$ T cells had incorporated BrdU in chimeric mice (Fig. 3 C). These findings indicate that dermal $\gamma\delta$ T cells are maintained through their local proliferation in steady-state conditions.

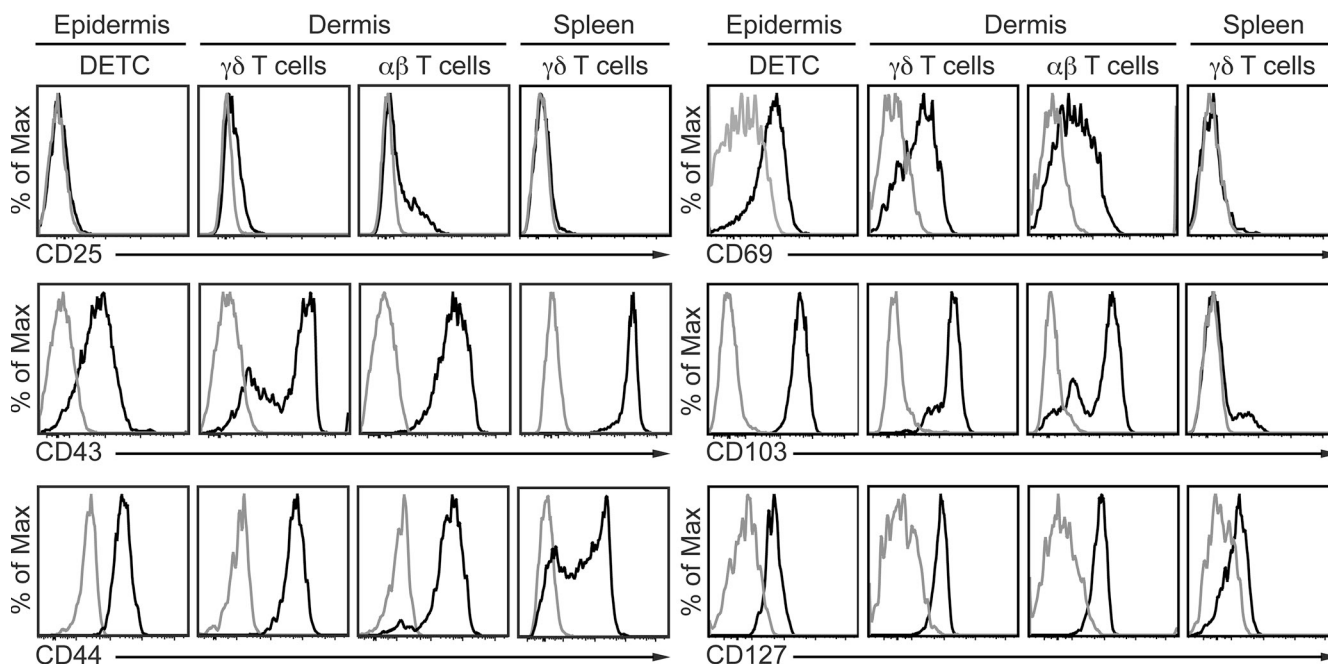


Figure 2. Phenotypic analyses of dermal $\gamma\delta$ T cells. Histograms of surface markers expressed by cutaneous and splenic $\gamma\delta$ T cells from WT mice ($n \geq 3$ per group). Histograms were pregated on CD45⁺MHC-II⁺CD3⁺ cells before gating on $\gamma\delta^+$ and $\gamma\delta^-$ T cell populations. Expression of the indicated markers is also shown for DETCs, dermal $\alpha\beta$ T cells, and splenic $\gamma\delta$ T cells. Gray lines, isotype control staining; black lines, indicated antibodies. Data are representative of at least two independent experiments.

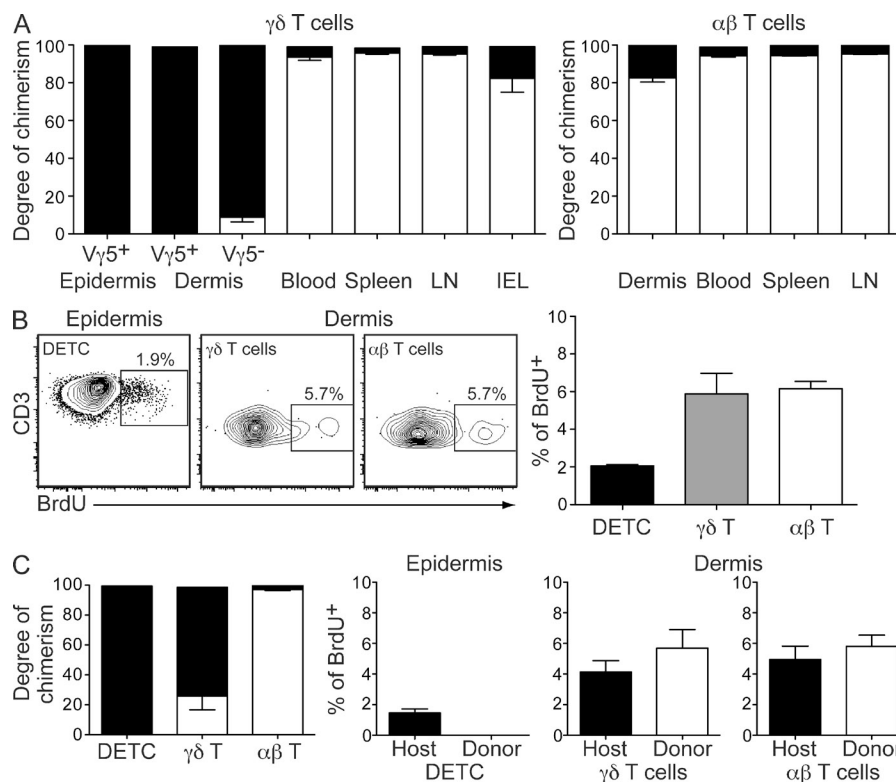


Figure 3. Dermal $\gamma\delta$ T cells are predominantly radioresistant and proliferate locally in the skin. (A) Degree of chimerism of $\gamma\delta$ T cells (left) and $\alpha\beta$ T cells (right) in various organs obtained 12 wk after reconstituting lethally irradiated WT mice with CD45.1 congenic bone marrow. Filled bars, host CD45.2; open bars, donor CD45.1. (B, left) Flow cytometry profiles of BrdU incorporation by epidermal and dermal T cells isolated from WT mice ($n \geq 5$ /group) 6 d after initial BrdU administration. (right) Frequency of cutaneous BrdU+ T cells 6 d after initial BrdU administration in WT mice ($n = 5$). (C, left) Degree of chimerism of cutaneous T cells obtained 19 mo after reconstitution ($n = 8$; chimeras generated as described in A). Right, percentage of host- or donor-derived epidermal and dermal T cells that are BrdU+ in chimeric mice 6 d after initial BrdU administration ($n = 8$). Data are representative of two to four independent experiments.

dermal $\gamma\delta$ T cells display a unique profile of cytokine dependence.

CXCR6^{EGFP} mice enable visualization of cutaneous $\gamma\delta$ T cells

We have previously demonstrated differential migratory behavior of LCs and DDCs in the ear skin of mice (Ng et al., 2008), i.e., LCs were found to be sessile, whereas DDCs were constitutively migratory. To test whether similar migratory behavior of cutaneous $\gamma\delta$ T cells could be observed, we made use of mice with an EGFP knock-in in the Bonzo/CXCR6 locus (CXCR6^{EGFP} mice; Unutmaz et al., 2000). In these mice, CD3+ T cell subsets, including NKT cells, effector and memory CD4+ and CD8+ $\alpha\beta$ T cells, and $\gamma\delta$ T cells express EGFP (Unutmaz et al., 2000). To evaluate EGFP expression in skin T cells, we analyzed single-cell suspensions prepared from separated epidermis and dermis of heterozygous CXCR6^{EGFP/+} (CXCR6^{EGFP}) mice by flow cytometry (Fig. 5 A). All DETCs, but not LCs, expressed high levels of EGFP (Fig. 5 A). Similarly, all dermal $\gamma\delta$ T cells were EGFP^{hi} (Fig. 5 A). In contrast, only a subset of $\alpha\beta$ T cells (10–40%) expressed EGFP, thereby accounting for 5–15% of EGFP+ dermal cells. $\gamma\delta$ T cells can express several chemokine receptors (Glatzel et al., 2002). However, unlike a role for CCR9 in tissue homing of $\gamma\delta$ T cells, studies in CXCR6-deficient mice do not demonstrate an obvious phenotype (Unutmaz et al., 2000). Consistently, we did not find any difference in number or phenotype of $\gamma\delta$ T cells in homozygous CXCR6^{EGFP/EGFP} mice, indicating that this chemokine receptor is not required for the trafficking of these cells to the skin (Fig. S2).

Next, we investigated the distribution of EGFP+ T cells in the skin by performing multiphoton imaging of the ear skin of CXCR6^{EGFP} mice (Fig. 5 B). Using second harmonic generation signals, we were able to distinguish between the extracellular matrix-free epidermis and the collagen-rich dermis (blue

Differential cytokine requirements for epidermal and dermal $\gamma\delta$ T cells

Based on the finding of in situ turnover of dermal $\gamma\delta$ T cells, we wondered which survival cytokines were controlling their development/maintenance. Epidermal V γ 5+ $\gamma\delta$ T cells have been shown to require both IL-7 and IL-15 for development and/or survival in vivo (Moore et al., 1996; Laky et al., 1998; De Creus et al., 2002). To determine whether dermal $\gamma\delta$ T cells had similar requirements, we tested IL-7^{-/-} and IL-15^{-/-} mice for the presence of these cells. Both DETCs and dermal $\gamma\delta$ T cells were dependent on IL-7 because IL-7^{-/-} mice were completely devoid of DETCs, and both the frequency and the number of dermal $\gamma\delta$ T cells (V γ 5- TCR $\gamma\delta$ +) were significantly reduced (Fig. 4). Thymi of IL-7^{-/-} mice were completely devoid of $\gamma\delta$ T cells, whereas the dermis still maintained a minor population of V γ 4- $\gamma\delta$ T cells (Fig. S1). This indicates that a subset of dermal $\gamma\delta$ T cells is IL-7-independent. The frequency of $\alpha\beta$ T cells remained unchanged, but the absolute number of cells was significantly reduced in IL-7^{-/-} mice compared with WT mice (Fig. 4, B and C). In contrast to DETCs, however, the frequency and the number of dermal $\gamma\delta$ T cells were unaltered in IL-15^{-/-} mice compared with WT mice (Fig. 4, B and C). Although the frequency of $\alpha\beta$ T cells remained unchanged in IL-15^{-/-} mice compared with WT mice, the number of cells was significantly reduced (Fig. 4, B and C). To further test the influence of IL-7 on dermal $\gamma\delta$ T cells, we evaluated their frequency in mice with transgenic overexpression of IL-7 (IL-7Tg; Mertsching et al., 1995). As shown in Fig. 4 C, this led to a significant increase in the number of dermal $\gamma\delta$ and $\alpha\beta$ T cells, but not DETCs. Therefore,

signal in Fig. 5 B). Vertical scans of the ear skin revealed a network of EGFP⁺ cells localized to the epidermis ~20 μ m below the stratum corneum. These cells exhibited long dendrites, characteristic of DETCs (Bergstresser et al., 1983; Tschachler et al., 1983). In the superficial dermis, we detected numerous EGFP⁺ cells that were morphologically different to the DETCs (Fig. 5 B). These cells were mostly round or amoeboid in shape with no visible dendrites (Fig. 5 B). The overall density of DETCs was greater than that of dermal EGFP⁺ T cells (Fig. 5 B).

Because in these studies we were unable to distinguish between dermal EGFP-expressing $\gamma\delta$ and $\alpha\beta$ T cells, we

crossed the CXCR6^{EGFP} mice onto a TCR β knockout background lacking all $\alpha\beta$ T cells (Fig. 5, C and D). Phenotype, density, and morphology of skin $\gamma\delta$ T cells in these mice were identical to CXCR6^{EGFP} mice (Fig. 5, C and D, and not depicted). These mice allowed us to further interrogate the migratory behavior of cutaneous $\gamma\delta$ T cells using time-lapse in vivo multiphoton microscopy in ear skin. Similarly to DCs, DETCs were sessile (mean migratory velocity <1 μ m/min; Fig. 5 E; Ng et al., 2008). Dermal EGFP⁺ $\gamma\delta$ T cells exhibited variable migratory behavior, with some cells migrating and others remaining sessile (mean velocity of 2.0 ± 0.3 μ m/min;

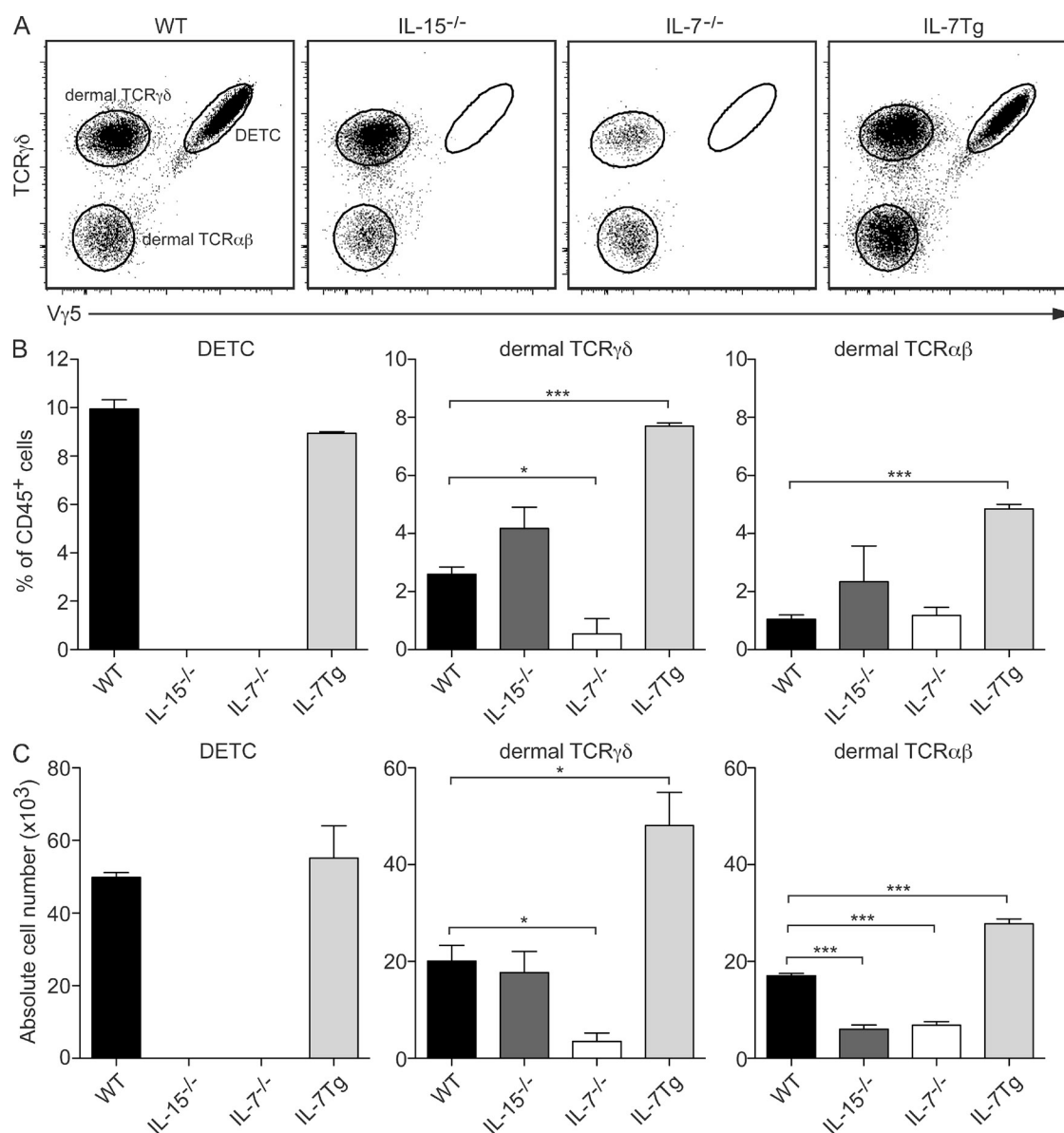


Figure 4. Epidermal and dermal $\gamma\delta$ T cells exhibit differential cytokine requirements for development/maintenance. (A) Flow cytometry profiles of cutaneous T cells isolated from WT, IL-15^{-/-}, IL-7^{-/-}, and IL-7Tg mice ($n \geq 3$ /group). Cells were gated on CD45⁺ CD3⁺. (B) Percentage of DETCs, dermal $\gamma\delta$ T cells, and $\alpha\beta$ T cells in the CD45⁺ leukocyte population in the ear skin of the various groups of mice. (C) Absolute numbers of DETCs, dermal $\gamma\delta$ T cells, and $\alpha\beta$ T cells in the ear skin of the various groups of mice. Data are representative of two to three independent experiments with at least three mice per group.

Fig. 5 E). Based on these results, we speculated that dermal $\gamma\delta$ T cells may reside in specific niches within the skin. Indeed, confocal microscopy in dermal sheets from $\text{TCR}\beta^{-/-}\text{xCXCR6}^{\text{EGFP}}$ mice demonstrated that a proportion of dermal $\gamma\delta$ T cells ($31 \pm 4.5\%$) physically associated with MHC II⁺ cells (Fig. 5 F). These data demonstrate that dermal $\gamma\delta$ T cells interact with their surroundings under steady-state conditions, which may indicate an immunoregulatory function for these cells.

Dermal $\gamma\delta$ T cell numbers are normal in CCR7-deficient animals

CCR7 is a crucial regulator of $\alpha\beta$ T cell exit from peripheral tissues via migration into lymphatic vessels (Bromley et al., 2005; Debes et al., 2005). To determine whether this is also

the case for $\gamma\delta$ T cells, we analyzed their numbers in CCR7-deficient mice. Consistently, a significant increase in $\alpha\beta$ T cell numbers was observed in the dermis of $\text{CCR7}^{-/-}$ mice compared with WT mice (Fig. 6). In contrast, the number of both DETCs and dermal $\gamma\delta$ T cells remained unchanged (Fig. 6). In skin-draining LN, however, both $\alpha\beta$ and $\gamma\delta$ T cells were reduced in numbers, consistent with a requirement of circulating T cells for CCR7 to traffic to LNs (Fig. 6). These data suggest that, unlike memory $\alpha\beta$ T cells, dermal $\gamma\delta$ T cells do not exit the skin under homeostatic conditions.

Antigen-specific CD4⁺ T cell priming is reduced in $\gamma\delta$ T cell-deficient mice

Having identified and characterized a population of resident $\gamma\delta$ T cells in the mouse dermis, we next sought to demonstrate

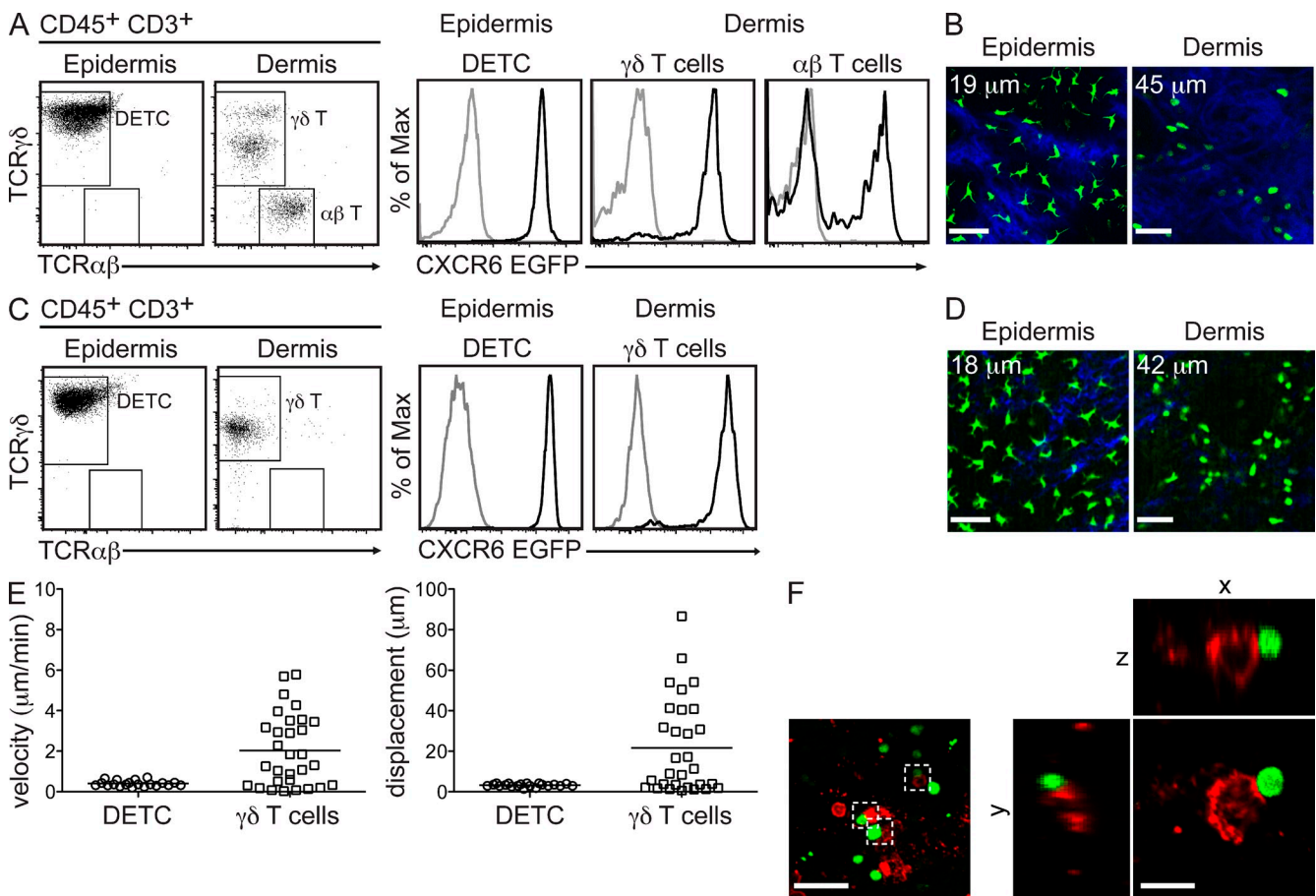


Figure 5. Real-time imaging of EGFP⁺ $\gamma\delta$ T cells in ear skin of $\text{TCR}\beta^{-/-}\text{xCXCR6}^{\text{EGFP}}$ mice. (A) Flow cytometry profiles of epidermal and dermal $\gamma\delta$ and $\alpha\beta$ T cells isolated from ear skin of CXCR6^{EGFP} mice ($n \geq 4$ mice/group). Histograms display the level of EGFP expression (black histogram, CXCR6^{EGFP} mice; gray histogram, WT mice). (B) Single-plane images from MP-IVM showing EGFP⁺ T cells in ear skin of CXCR6^{EGFP} mouse at two different vertical depths (indicated by the number in the top left corner) along the z-projection. Bars, 31 μm . (C) Flow cytometry profiles of epidermal and dermal $\gamma\delta$ T cells isolated from ear skin of $\text{TCR}\beta^{-/-}\text{xCXCR6}^{\text{EGFP}}$ mice ($n \geq 4$ mice/group). Histograms display the level of EGFP expression by epidermal and dermal $\gamma\delta$ T cells (black histogram, $\text{TCR}\beta^{-/-}\text{xCXCR6}^{\text{EGFP}}$ mice; gray histogram, WT mice). (D) Single-plane images from MP-IVM showing EGFP⁺ DETCs and dermal $\gamma\delta$ T cells in ear skin of $\text{TCR}\beta^{-/-}\text{xCXCR6}^{\text{EGFP}}$ mouse at two different vertical depths (indicated by the number in the top left corner) along the z-projection. Bars, 31 μm . (E) Mean migratory velocity (left) and displacement (right) of DETCs and dermal $\gamma\delta$ T cells from 20-min tracks ($n > 20$ cells; symbols represent individual cells) in $\text{TCR}\beta^{-/-}\text{xCXCR6}^{\text{EGFP}}$ mice. (F) Single-plane and three-dimensional images from dermal whole-mount stains depicting dermal EGFP⁺ $\gamma\delta$ T cells in contact with MHC II⁺ cells in ear skin of $\text{TCR}\beta^{-/-}\text{xCXCR6}^{\text{EGFP}}$ mice. Bars: (left) 38 μm ; (right) 13 μm . Data are representative of two to three independent experiments.

a role for these cells in immune responses. To do this, we made use of a *Mycobacterium bovis* Bacille Calmette-Guérin (BCG) infection model because $\gamma\delta$ T cells have been previously reported to play a role in immunity to mycobacteria (Hayday, 2009; Cua and Tato, 2010). As a readout, we measured the expansion of antigen-specific T cells in the retroauricular LNs after intradermal (i.d.) BCG infection of ear skin. WT and TCR $\delta^{-/-}$ mice were adoptively transferred with CFSE-labeled P25-TCR transgenic CD4 $^{+}$ T cells, which recognize an immunodominant epitope (peptide 25) from *Mycobacterium tuberculosis* antigen 85B (Tamura et al., 2004). 24 h later, mice were infected with a low dose of BCG (10^5 CFU). At days 5 and 6 after infection, BCG in TCR $\delta^{-/-}$ mice induced significantly lower expansion of CD44 $^{+}$ CFSE $^{lo/-}$ P25 T cells as compared with WT mice (Fig. 7 A). Because TCR $\delta^{-/-}$ mice not only lack $\gamma\delta$ T cells in the skin but in all organs, it remained possible that the observed difference in CD4 $^{+}$ T cell expansion was caused by the absence of $\gamma\delta$ T cells in draining LN rather than in the skin. To address this question, we investigated the P25 T cell response to intraperitoneal BCG infection, in which dermal $\gamma\delta$ T cells would not be involved. At day 6 after infection, no difference in the expansion of P25 CD4 $^{+}$ T cells was observed between WT and TCR $\delta^{-/-}$ mice (Fig. 7 B). These data suggested that cutaneous $\gamma\delta$ T cells rather than circulatory $\gamma\delta$ T cells regulated the downstream CD4 $^{+}$ T cell response

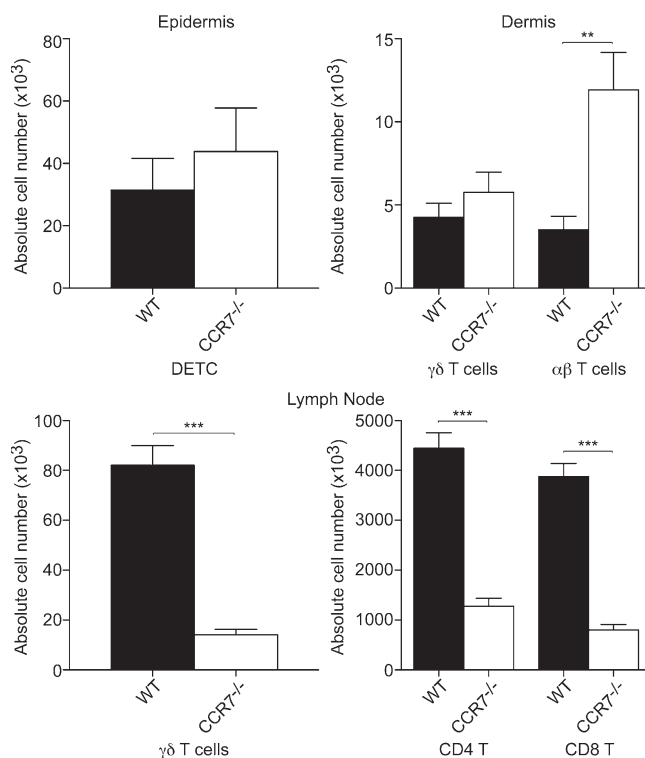


Figure 6. Effect of CCR7 deficiency on T cell numbers in the skin and LN. Absolute numbers of $\gamma\delta$ T cells and $\alpha\beta$ T cells in the ear skin and peripheral LN of WT and CCR7^{-/-} mice ($n \geq 8$ per group) under steady-state conditions. Data are representative of three independent experiments. Data are presented as mean \pm SEM.

to skin challenge. Because in this model the pathogen was directly introduced into the dermis, and thus physically separated from DETCs, our data further suggest that dermal $\gamma\delta$ T cells play the major, if not exclusive, role in this effect. In addition, we found a subtle but significant up-regulation of the early activation marker CD69 on dermal $\gamma\delta$ T cells, but not DETCs, 24 h after BCG infection (Fig. S3).

Early recruitment of neutrophils to sites of BCG infection is compromised in $\gamma\delta$ T cell-deficient mice

Several mechanisms may underlie the observed deficiency in T cell expansion in TCR $\delta^{-/-}$ mice. For example, $\gamma\delta$ T cells may influence DC development and/or maturation. We therefore examined the frequencies and absolute numbers of conventional and migratory DCs in TCR $\delta^{-/-}$ mice, but observed no differences to WT controls (unpublished data). To test whether skin DCs could be adequately activated in the absence of $\gamma\delta$ T cells, we analyzed the expression of co-stimulatory molecules by DCs after subcutaneous immunization with CFA. Expression of CD80 and CD86 by DC from both WT and TCR $\delta^{-/-}$ mice was comparable at day 3 after CFA administration (Fig. S4), indicating normal activation of these cells in the absence of $\gamma\delta$ T cells.

Some subsets of $\gamma\delta$ T cells are potent producers of the proinflammatory cytokine IL-17 and, based on this function, have been implicated in the recruitment of neutrophils in response to bacterial pathogens including *E. coli* and *Staphylococcus aureus* (Shibata et al., 2007; Cho et al., 2010; Cua and Tato, 2010). Given that cutaneous $\gamma\delta$ T cells are well positioned to respond rapidly to skin invading pathogens, we examined whether these cells were capable of producing IL-17 after i.d. infection with BCG. As shown in Fig. 8 (A and B), ~6% of dermal $\gamma\delta$ T cells secreted IL-17 rapidly after i.d. BCG inoculation, whereas both DETCs and $\alpha\beta$ T cells exhibited very low IL-17 production.

Next, we determined neutrophil infiltration in the skin after i.d. infection with BCG in WT and TCR $\delta^{-/-}$ mice. Consistent with previously reported findings (Abadie et al., 2005), we observed a rapid infiltration of Gr1 $^{+}$ neutrophils in the skin of WT mice after infection with BCG, which reached a peak at 24 h after infection (Fig. 9, A and B). Confocal imaging of whole-mount dermal sheets revealed that Gr1 $^{+}$ neutrophils clustered around the i.d. BCG deposit, and were frequently found to contain intracellular mCherry-tagged bacteria (Fig. 9 A). Importantly, BCG-containing neutrophils were detected in dermal lymphatic vessels, indicating their role in bacteria transport to draining LN (Fig. 9 A; Abadie et al., 2005). Using flow cytometry, we determined that neutrophils were the predominant leukocyte population ($83 \pm 1.8\%$) to have internalized BCG at this early time point (Fig. 9 A), whereas the rest of BCG-containing cells were MHC II lo cells, which are most likely macrophages. DDCs represented only a minor population of cells to pick up BCG (~1%).

When we then compared the recruitment of neutrophils in BCG-infected TCR $\delta^{-/-}$ mice, we observed a significant decrease in the number of neutrophils accumulating in the

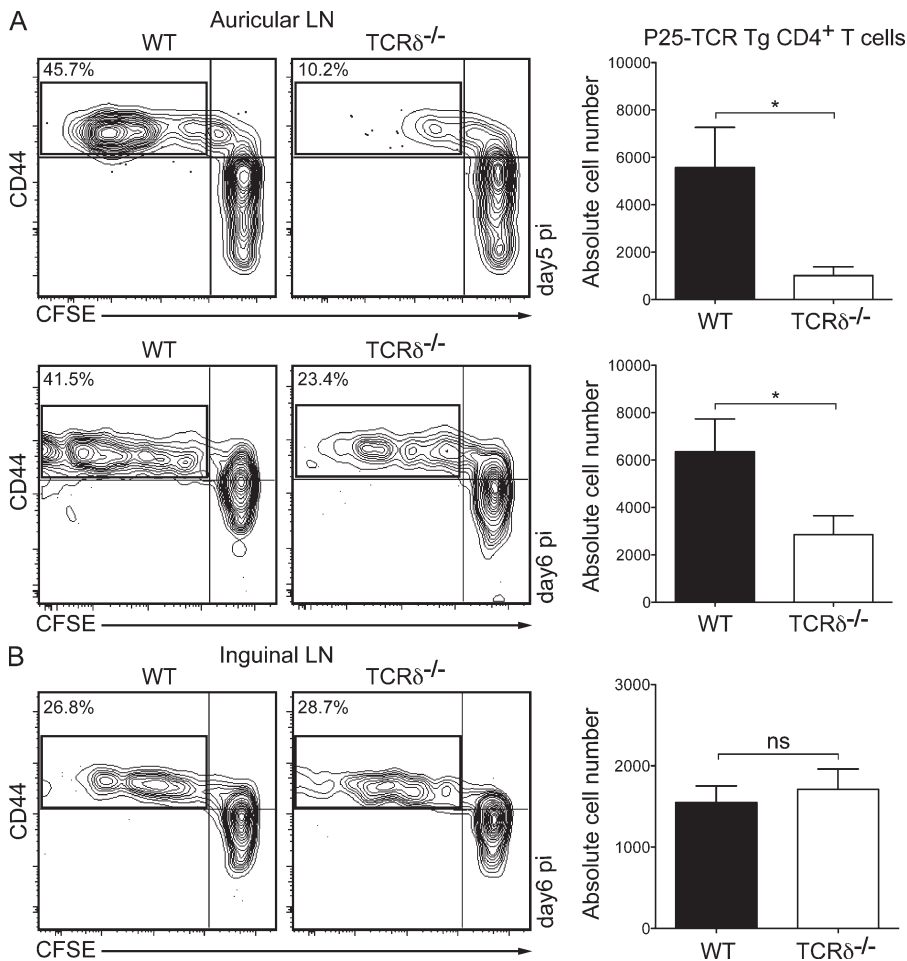


Figure 7. Antigen-specific CD4⁺ T cell response to BCG infection is decreased in TCRδ^{-/-} mice. (A, left) Flow cytometry profiles of CFSE-labeled P25 transgenic CD4⁺ T cells recovered from auricular LN of WT and TCRδ^{-/-} mice, 5 or 6 d after i.d. infection with 10⁵ CFU BCG ($n = 4-9$ /group). Data are representative of 1 (day 5 after infection) to 3 (day 6 after infection) independent experiments. (right) Absolute numbers of CD44⁺CFSE^{lo/-} P25 CD4⁺ T cells (indicated by the box in the top left quadrant; left) recovered from auricular LN. (B, left) Flow cytometry profiles of CFSE-labeled P25 transgenic CD4⁺ T cells recovered from inguinal LN of WT and TCRδ^{-/-} mice, 6 d after i.p. infection with 10⁵ CFU BCG ($n = 7$ /group). Data are representative of two independent experiments. (right) Absolute number of CD44⁺CFSE^{lo/-} P25 transgenic CD4⁺ T cells (indicated by the box, left) recovered from inguinal LN. Data are presented as mean \pm SEM.

skin of TCRδ^{-/-} mice at 24 h after infection compared with WT controls (Fig. 9 C). This decrease was not caused by differences in the number of neutrophils in circulation in WT and TCRδ^{-/-} mice in the steady-state (unpublished data). Importantly, using quantitative RT-PCR, we found a significantly lower amount of BCG in the draining LN of TCRδ^{-/-}

mice at day 3 after infection compared with WT controls (Fig. 9 D), indicating impaired antigen transport via lymphatic vessels. Together, these data show that dermal $\gamma\delta$ T cells are the predominant source of IL-17 in the skin after BCG infection and that these cells regulate the composition of the cutaneous inflammatory infiltrate under these conditions.

DISCUSSION

The skin represents the outermost defense against microbial and environmental insults. The importance of cutaneous integrity is emphasized by the multitude of strategies that counteract pathogen invasion, including the physical barrier provided by keratinocytes, the production of antimicrobial

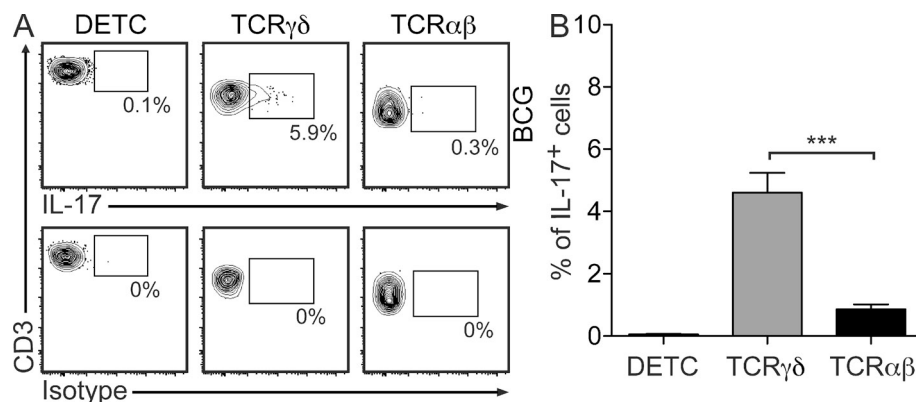


Figure 8. Dermal $\gamma\delta$ T cells are the predominant source of IL-17 in the skin after BCG infection. (A) Flow cytometry profiles of IL-17-producing cutaneous T cells isolated from ear skin of WT mice ($n \geq 4$ /group) 24 h after i.d. infection with 10⁵ CFU BCG. Data are representative of five independent experiments. (B) Frequency of IL-17-producing cutaneous T cells isolated from ear skin of BCG-infected mice ($n = 11$).

mediators by skin-resident cells, and the localization of immune cells in the different layers of the skin. It has become increasingly clear that epidermis and dermis do not merely represent anatomically distinct compartments, but rather directly and specifically shape the immune milieu to support the activities of resident leukocytes. In this study, we have identified an abundant population of resident dermal $\gamma\delta$ T cells that displays a unique phenotypic profile, survival requirements, and migratory behavior as compared with its epidermal and systemic counterparts. Our results thus expand on the concept of microcompartmental specialization of distinct immune cell subsets within the skin. They further emphasize the need to define the function of dermal $\gamma\delta$ T cells in skin immunity and for the study of the environmental and molecular cues that regulate these cells during homeostatic and inflammatory conditions.

It is quite surprising that dermal $\gamma\delta$ T cells in the mouse have received little or no attention in the past, given that DETCs have served as a paradigm for studying $\gamma\delta$ T cell biology. Nakagawa et al. (1993) reported on the migration of $V\gamma 5^-$ $\gamma\delta$ T cells from whole-skin explants of mice, but did not further investigate their original localization. Tamaki et al. (1996) identified Thy-1^+ dermal cells of dendritic shape that expressed $V\gamma 5$; however, these cells also contained melanosomes and therefore may have represented autofluorescent dermal macrophages. In mice with transgenic IL-7 overexpression in basal keratinocytes, increased numbers of cutaneous $\gamma\delta$ and $\alpha\beta$ T cells were observed (Williams et al., 1997). The authors speculated that this increase may have been caused by an expansion of precursor cells present within the dermis, but did not characterize these cells any further. More recently, Kisielow et al. (2008) reported on the presence of

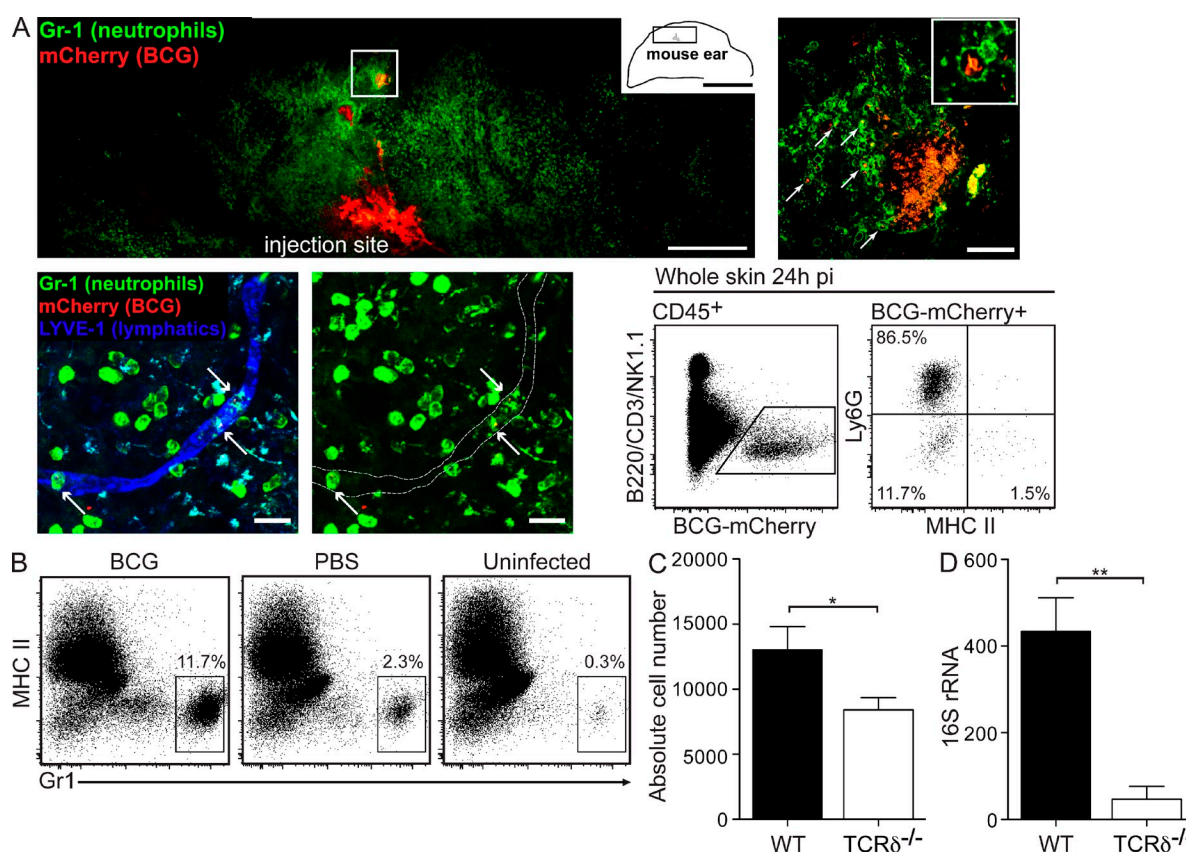


Figure 9. Neutrophil recruitment to the site of BCG infection is compromised in the absence of IL-17-producing $\gamma\delta$ T cells. (A, top left) Single-plane image from a dermal whole-mount stain depicting Gr1^+ neutrophils at the site of BCG infection in ear skin of WT mice 24 h after infection. Bar, 500 μm . (top right) higher magnification of the boxed area in the top left panel depicting Gr1^+ neutrophils around a deposit of BCG. Arrows point to BCG-containing Gr1^+ neutrophils. Boxed inset shows a single Gr1^+ neutrophil containing intracellular BCG bacilli. Bar, 50 μm . (bottom left) Extended focus image from a dermal whole-mount stain 36 h after BCG infection depicting BCG-incorporated Gr1^+ neutrophils (arrows) in the lumen of a lymphatic vessel stained with anti-LYVE-1. Bars, 25 μm . (bottom right) Flow cytometry profiles of CD45^+ leukocytes isolated from WT ear skin, 24 h after i.d. infection with BCG-mCherry. CD45^+ BCG-mCherry $^+$ cells were further evaluated for Ly6G and MHC II expression. Data are representative of two to four independent experiments. (B) Flow cytometry profiles of Gr1^+ cells infiltrating the skin of WT mice ($n = 4$), 24 h after i.d. injection with BCG or PBS. Cells were gated on CD45^+ CD3^- . Data are representative of 3 independent experiments. (C) Absolute cell number of Gr1^+ neutrophils isolated from ear skin of WT and $\text{TCR}\delta^{-/-}$ mice ($n = 14$ –17 per group), 24 h after i.d. infection with BCG. Data are representative of three independent experiments. (D) Copy number of 16S rRNA from BCG isolated from auricular draining LN of WT and $\text{TCR}\delta^{-/-}$ mice ($n = 5$ per group), 3 d after i.d. infection. Data are representative of two independent experiments.

SCART2⁺V γ 5⁻ $\gamma\delta$ T cells in the dermis. However, no further phenotypic or functional characterization of the dermal population was performed. Human dermis has been reported to contain an oligoclonal population of $\gamma\delta$ T cells that differs in their TCR repertoire from circulating $\gamma\delta$ T cells (Bos et al., 1990; Foster et al., 1990; Holtmeier et al., 2001). Our data support the concept of oligoclonality demonstrated by the broader repertoire of TCRs expressed by murine dermal $\gamma\delta$ T cells as compared with DETCs, suggesting that they are capable of responding to a more diverse spectrum of antigens. Therefore, the predominant function of DETCs may be their role as “lymphoid stress-sensors” (Hayday, 2009), that is the recognition of self-encoded stress molecules on keratinocytes upon epithelial disturbance such as trauma or epidermal infection. Dermal $\gamma\delta$ T cells on the other hand, may act as direct pathogen sensors that rapidly respond to foreign antigens upon their introduction into the dermis. The immediate production of proinflammatory cytokines, most prominently IL-17, then triggers an inflammatory cascade to facilitate clearance of the pathogen. Clearly, future studies will need to further dissect the role individual $\gamma\delta$ T cell subpopulations play after the introduction of pathogens, including bacteria, fungi or viruses, into the epithelium or dermis.

Another novel finding in this study is the capacity of dermal $\gamma\delta$ T cells to proliferate in situ. Strikingly, in chimeric mice, 80% of these cells were still host derived even 19 mo after bone marrow reconstitution, indicating that the dermal $\gamma\delta$ T cell population is largely self-renewing under homeostatic conditions. These data contrast with the paradigm of cutaneous $\alpha\beta$ T cell immunosurveillance, which has traditionally been believed to occur by means of continuous trafficking of circulating cells through the skin. Thus, antigen-experienced $\alpha\beta$ T cells expressing skin homing receptors, such as E-selectin ligands, enter the skin and, in the absence of antigen, exit in a CCR7-dependent manner via lymphatics (Yoshida et al., 1998; Bromley et al., 2005; Debes et al., 2005). Consistently, we found that cutaneous $\alpha\beta$ T cells are replaced in bone marrow chimeras, indicating different survival signals for dermal $\alpha\beta$ and $\gamma\delta$ T cells. The difference in screening behavior of the two T cell subsets is further corroborated by the fact that dermal $\gamma\delta$ T cells exhibited very little interstitial migration. Although we did not visualize dermal $\alpha\beta$ T cells in our system, previous studies have shown that naive $\alpha\beta$ T cells in the LN and effector/memory T cells in peripheral tissues, including the skin, migrate at much higher velocities (~ 10 $\mu\text{m}/\text{min}$) in the absence of cognate signals than dermal $\gamma\delta$ T cells (Miller et al., 2002; Mrass et al., 2006; Matheu et al., 2008). This difference may be at least partly accounted for by the observation that one third of dermal $\gamma\delta$ T cells were in close contact with MHC II⁺ cells. Interactions between $\gamma\delta$ T cells and MHC II⁺ cells have previously been found in the lungs (Wands et al., 2005). Although we do not know the molecular basis of these interactions, it is conceivable that dermal $\gamma\delta$ T cells recognize self-antigens on APCs. In this context, it is interesting to note that TCR $\delta^{-/-}$ mice develop spontaneous dermatitis, at least on certain genetic backgrounds

(Girardi et al., 2002). Thus, the APC- $\gamma\delta$ T cell crosstalk in the dermis under noninflammatory conditions may serve an immunoregulatory function.

At the functional level, we have found that cutaneous $\gamma\delta$ T cells regulate the downstream CD4⁺ T cell response to i.d. BCG infection. These results are in line with previous studies demonstrating that $\gamma\delta$ T cells are involved in protective immunity against mycobacterial infections (Hayday, 2009; Cua and Tato, 2010). Importantly, our experiments suggest that dermal $\gamma\delta$ T cells are the predominant source of IL-17 in the skin, whereas DETCs displayed negligible production. Our findings are somewhat in contrast with a recent study that demonstrated IL-17 production by DETCs in the skin after *S. aureus* infection (Cho et al., 2010). Despite the fact that *S. aureus* was applied i.d., dermal cells produced considerably less IL-17 than epidermal cells. However, this study did not use single-cell labeling, but rather determined IL-17 levels in the entire CD3⁺ dermal and epidermal populations after in vitro restimulation for 24 h. In our experience, dermal $\gamma\delta$ T cells die within a few hours after their isolation, which may be a confounding factor for the analysis of culture supernatants. Finally, it is possible that Gram-positive cocci and mycobacteria induce different response programs in dermal $\gamma\delta$ T cells. In sum, we show that dermal $\gamma\delta$ T cells resemble the previously described subset of “innate” $\gamma\delta$ T cells defined by their production of IL-17 (Jensen et al., 2008; Shibata et al., 2008; Ribot et al., 2009). Future studies will focus on determining the full profile of cytokines, chemokines, and other mediators produced by these cells in response to pathogens.

IL-17 has been implicated in the recruitment of neutrophils to sites of infection and inflammation (Kolls and Lindén, 2004; Lindén et al., 2005; Cua and Tato, 2010), and our data showed that neutrophil recruitment was decreased in TCR $\delta^{-/-}$ mice in response to i.d. BCG infection. Neutrophils have previously been shown to be the first blood-borne cells to arrive at the site of dermal BCG infection in mice, where they subsequently “pick up” and shuttle live bacilli to the skin-draining LN (Abadie et al., 2005). Because DC numbers and phenotype were identical in WT and TCR $\delta^{-/-}$ mice, a likely mechanism for the reduced priming of mycobacteria-specific CD4⁺ T cells in TCR $\delta^{-/-}$ mice is the decreased availability of antigen in LNs caused by decreased neutrophil trafficking. In addition, because IL-17 also activates neutrophils, the reduced availability of this cytokine may also influence the phagocytic capacity of these cells. Indeed, BCG was much less abundant in the draining LN of TCR $\delta^{-/-}$ mice, most likely relating to decreased antigen transport by neutrophils via dermal lymphatic vessels. Future studies will evaluate the distribution of fluorescently tagged BCG in draining LNs, as well as the capacity of DCs to activate antigen-specific T cells.

Collectively, dermal $\gamma\delta$ T cells emerge as new players in the regulation of skin homeostasis and immunity. Although we have identified one of their functions, namely the response to mycobacterial infection, it remains to be determined whether they fulfill roles similar to those ascribed to DETCs

during wound repair and surveillance for stressed and tumor cells. Nevertheless, it is conceivable that some of the activities previously attributed to DETCs may in fact be performed by their dermal cousins.

MATERIALS AND METHODS

Mice. C57BL/6 (WT) and B6.SJL/Ptpr^a (CD45.1) mice were purchased from the Animal Research Centre (Perth, Australia). Peptide-25 TCR transgenic (P25 TCR-Tg) mice have been described previously (Tamura et al., 2004). IL-7^{-/-}, IL-15^{-/-}, and IL-7 transgenic (IL-7Tg) mice were provided by J.H. Cho and J. Sprent (Garvan Institute, Sydney, Australia). CXCR6^{EGFP}, CCR7^{-/-}, TCRδ^{-/-}, and TCRβ^{-/-} mice were purchased from The Jackson Laboratory. All mice used were on a C57BL/6 background and between 8 and 16 wk of age. All mouse strains, excluding IL-7^{-/-}, IL-15^{-/-}, and IL-7Tg mice, were bred and maintained in specific pathogen-free conditions at the Centenary Institute animal facility. All animal experiments were performed with the approval of the Animal Ethics Committee at the University of Sydney.

Generation of bone marrow chimeras. To create bone marrow chimeras, C57BL/6 (CD45.2) hosts were lethally irradiated with 1,200 cGy split-dose irradiation (2 doses of 600 cGy each, 4 h apart). 24 h later, the irradiated hosts received 8–10 × 10⁶ bone marrow cells from B6.SJL/Ptpr^a (CD45.1) donor mice intravenously via the tail vein. Chimeric mice were given a course of antibiotics in sterile drinking water for 3 wk after irradiation to prevent infections. All chimeric mice were allowed to reconstitute for at least 3 mo before use in experiments.

Tissue processing and flow cytometry. Isolation of skin cells involved the following process. Ears were split into dorsal and ventral halves using forceps and subjected to enzymatic digestion as follows: first step, 5 U/ml dispase I (BD) in PBS for 90 min at 37°C to allow for epidermal and dermal separation; second step, 2 mg/ml collagenase type IV (Sigma-Aldrich) in PBS for 45 min at 37°C to release cells. In certain experiments where cell surface markers of interest were dispase sensitive and would potentially be cleaved, ears were only digested with 2 mg/ml collagenase type IV in PBS for 60 min at 37°C. To obtain single-cell suspensions, the tissues were filtered through an 80-μm stainless steel mesh. Isolation of leukocytes from the spleen and LN involved teasing the organs apart, followed by filtering through an 80-μm stainless steel mesh to obtain single-cell suspensions.

Single-cell suspensions were incubated with anti-CD16/32 (2.4G2; BD) to block Fc receptors and stained with fluorochrome-conjugated antibodies diluted in "FACS buffer" (PBS containing 5% FCS, 2 mM EDTA, and 0.02% sodium azide). Fluorochrome-conjugated antibodies (purchased from BD, eBioscience, or BioLegend) against the following cell surface molecules were used: CD3 (145-2C11), CD4 (RM4-5), CD8 (53-6.7), CD25 (PC61), CD43 (S7), CD44 (IM7), CD45 (30-F11), CD45.1 (A20), CD45.2 (104), CD69 (H1.2F3), CD80 (16-10A1), CD86 (GL1), CD103 (2E7), CD127 (A7R34), B220 (RA3-6B2), Gr1 (RB6-8C5), Ly6G (1A8), MHC II (M5/114), TCRβ (H57-597), TCRγδ (GL3), Vγ5 (536), and Vγ4 (UC3-10A6). After staining, cell suspensions were resuspended in FACS buffer containing 0.5 μg/ml DAPI (Invitrogen) for dead cell exclusion. For intracellular anti-BrdU staining, samples were first stained for cell surface molecules and aquafluorescent reactive dye (Invitrogen) for dead cell exclusion after fixation. Samples were acquired using an LSR-II flow cytometer (BD) and data were analyzed using FlowJo software (Tree Star, Inc.).

BrdU labeling in vivo. Mice were injected i.p. with 1 mg BrdU (BD) to ensure its immediate availability, and then given 0.8 mg/ml BrdU in sterile drinking water that was changed daily. Epidermal and dermal cell suspensions were prepared at day 6 after initial BrdU administration. Cell suspensions were stained for surface markers as described in the previous section, and BrdU⁺ cells were identified using the BrdU Flow kit (BD) according to the manufacturer's protocol.

P25-TCR transgenic CD4⁺ T cell isolation, labeling, and adoptive transfer. Spleens and LNs were harvested from P25-TCR transgenic mice and single-cell suspensions were obtained. Erythrocytes were osmotically lysed in NH₄Cl, and the cells were washed twice in RPMI 1640 (Invitrogen) supplemented with 10% FCS. CD4⁺ T cells were magnetically purified by negative selection using PE-conjugated anti-B220 (RA3-6B2), CD11b (M1/70), CD11c (HL3), NK1.1 (PK136), and TCRγδ (GL3) antibodies (BD or eBioscience) and anti-PE immunomagnetic beads (Miltenyi Biotec). CD4⁺ T cell purity was routinely >80% as assessed by flow cytometry. For proliferation assays, purified T cells were labeled with CFSE (Invitrogen) by resuspending the P25-TCR transgenic T cells in serum-free RPMI 1640 containing 5 μM CFSE. Cells were incubated with CFSE for 10 min at 37°C with intermittent mixing every 3–4 min. Labeling was stopped by adding ice-cold FCS and the cells were washed twice in RPMI 1640 with 10% FCS. WT and TCRδ^{-/-} host mice received 5 × 10⁵ CFSE-labeled P25-TCR transgenic CD4⁺ T cells intravenously via the tail vein.

BCG generation and infection. Fluorescently tagged BCG was generated as described previously (Triccas et al., 1999). Mice were anesthetized by i.p. injection of Ketamine/Xylazine (80/10 mg/kg), and 10⁵ CFU of BCG (in 2 μl saline) was injected i.d. into the pinnae of ears using a 35-gauge Hamilton syringe as described previously (Ng et al., 2008). For systemic infection, 10⁵ CFU of BCG (in 100 μl saline) was injected i.p. Ears were harvested at various time points after infection and analyzed by flow cytometry or confocal microscopy. Mice that received CFSE-labeled P25-TCR transgenic CD4⁺ T cells were infected 24 h after adoptive transfer of cells. On day 5 or 6 after infection, organs were harvested and analyzed by flow cytometry.

Cytokine secretion assay. 24 h after i.d. BCG (10⁵ CFU) infection, epidermal and dermal cells isolated from ear skin of mice (as described in Tissue processing and flow cytometry) were further stimulated ex vivo by culturing in RPMI 1640 containing 10% FCS, PMA (100 ng/ml), and Ionomycin (500 ng/ml) for 2 h at 37°C. IL-17 secretion by epidermal and dermal cells was analyzed using the Cytokine Secretion Assay Detection kit (Miltenyi Biotec) according to the manufacturer's protocol. Cell suspensions were then stained for surface markers as described above and analyzed by flow cytometry.

Quantitation of bacterial gene expression. WT and TCRδ^{-/-} mice were infected i.d. with 10⁵ CFU BCG, and 3 d after infection auricular draining LNs were isolated and resuspended in TRIZOL (Invitrogen). Cells were then disrupted by a Mini-Beadbeater-16 with 0.1 mm zirconia/silica beads (BioSpec Products). Homogenates were extracted with chloroform/isopropanol, and the pellet was resuspended in 100 μl of DEPC-treated water (Invitrogen). The solution was treated with TURBO DNase according to manufacturer's instructions (Applied Biosystems), and RNA was additionally purified by treatment with phenol/chloroform/isoamyl alcohol. Total RNA was dissolved in 20 μl of DEPC-treated water and stored at -80°C until needed.

For quantitation of *M. tuberculosis* gene expression, cDNA was prepared by reverse transcribing 1 μg of total RNA using a gene-specific primer (5'-GCCCCGACGCTCACAGTTAAG-3') for the mycobacterial house keeping gene 16S rRNA encoded by *rrs*, and Superscript III reverse transcription (Invitrogen) according to the manufacturer's recommendations. The number of *rrs* amplicons was measured by real-time PCR using the following primer pair; *rrs* forward 5'-AGGCAGCAGTGGGGAATA-3'; *rrs* reverse, 5'-CTACCGTCAATCCGAGAGAA-3'. 2 μl of cDNA, 6.25 μl SYBR green I PCR Master Mix (QIAGEN), and 5 μM of the *rrs* primer pair was added to each reaction to a total volume of 12.5 μl with DEPC-treated water. The reaction profile consisted of 50°C for 2 min and 95°C for 2 min, followed by 80 cycles at 95°C for 15 s, 55°C for 15 s, and 72°C for 15 s. PCR reactions were run on a Rotor-Gene 6000-series sequence detector (Rotor-gene; Corbett Life Science) and were performed in duplicate per sample. 10-fold dilutions of known amounts of plasmid DNA encoding *M. tuberculosis rrs* (7.2 × 10² to 7.2 × 10⁸ copies) were used to generate a standard curve. The copy number in each sample was calculated according to the formula $N = (Ct - b)/m$,

where N is the copy number, C_t is the threshold cycle, b is the y intercept, and m is the slope of the standard curve line.

Confocal microscopy of mouse ear dermis. Epidermis and dermis were separated as described in Tissue processing and flow cytometry, and the dermal half was fixed in 4% paraformaldehyde/10% sucrose for 30 min at room temperature. Fixed tissue was washed in PBS and blocked in 5% FCS in PBS for 2 h at room temperature. In some experiments, dermal tissue was treated with EDTA and Triton X as described previously (Chinnery et al., 2007) to increase antibody penetration. Subsequently, the tissue was incubated in purified anti-MHC II (IA/IE; BD), anti-LYVE-1 (R&D Systems), or anti-Gr1 (Ly6C/G; BD) for 60 min at room temperature or overnight at 4°C, washed, and counterstained with Alexa Fluor 647–conjugated goat anti-rat antibody, Alexa Fluor 647–conjugated donkey anti-goat antibody, or Alexa Fluor 488–conjugated goat anti-rat antibody (Invitrogen) for an additional 90 min. Tissues were thoroughly washed with PBS between all steps. Dermal tissues were then mounted on slides with anti-fade mounting solution (DABCO). Images were acquired on a Leica TCS SP5 confocal microscope system. Acquired image stacks were processed using Velocity software (Improvision).

Multiphoton intravital imaging of skin and image analysis. Preparation of animals and imaging was performed as previously described (Ng et al., 2008; Roediger et al., 2008). In brief, mice were anesthetized by i.p. injection of Ketamine/Xylazine (80/10mg/kg), with repeated half-dose injections as required. The ears were treated in brief with Nair solution (Church & Dwight) to remove hairs. The animals were then placed onto a custom-built stage to position the ear on a small metal platform for multiphoton (MP) imaging. The ear was immersed in PBS/glycerin (70:30, vol:vol) and covered with a coverslip. The temperature of the platform can be regulated independently, and was maintained at 36°C, whereas the body temperature was kept at 37°C using a heating pad placed underneath the mouse.

Multiphoton intravital microscopy was performed on a TriMScope (LaVision BioTec) attached to an Olympus BX-51 fixed stage microscope equipped with 20× (NA 0.95) and 40× (NA 0.8) water immersion objectives as previously described (Ng et al., 2008; Roediger et al., 2008). The samples were exposed to polarized laser light at a wavelength of 950 nm. Three-dimensional (x, y, z) images of the ear skin were acquired (1–6-μm spacing in z-axis over a total distance of 30–40 μm) every 30–60 s for a period of 1–2 h. Acquired image stacks were processed using Velocity software (Improvision). Migration parameters and cellular interactions were assessed as described (Mrass et al., 2006).

Immunization with CFA and DC isolation. WT and TCRδ^{−/−} mice were immunized s.c. in a hind footpad with CFA (Sigma-Aldrich; emulsified 1:1 in PBS; 40 μl/footpad). DCs were isolated 3 d post-immunization from draining popliteal and inguinal LN. In brief, LNs were digested in 2 mg/ml collagenase D (Roche) in PBS for 30 min at room temperature with gentle agitation. Single cell suspensions were obtained and stained for surface markers as described previously and analyzed by flow cytometry.

Statistical analysis. Data are presented as mean ± SEM. Student's t test or one-way analysis of variance were used to compare experimental groups. A difference was considered significant if $P < 0.05$.

Online supplemental material. Fig. S1 shows that although the dermis of IL-7^{−/−} mice contains a minor population of Vγ4⁺ γδ T cells, the thymus is completely devoid of both Vγ4⁺ and Vγ4[−] γδ T cells. Fig. S2 shows that CXCR6-deficient mice do not exhibit a difference in the number of cutaneous T cells compared with heterozygous CXCR6^{EGFP/+} mice. Fig. S3 shows that dermal γδ T cells are activated early after BCG infection. Fig. S4 shows that DC activation after inflammation is normal in TCRδ^{−/−} mice compared with WT mice. Online supplemental material is available at <http://www.jem.org/cgi/content/full/jem.20101824/DC1>.

We thank Dr. Adrian Hayday (King's College, London) for helpful discussion. We thank Dr. Jae Ho Cho and Prof. Jonathan Sprent (Garvan Institute, Sydney) for

providing knockout and transgenic IL-7 and IL-15 mouse strains and Prof. K. Takatsu (Institute of Medical Science, University of Tokyo) for provision of the p25 transgenic mice.

This work was supported by National Health and Medical Research Council grants 570769, 570742 (to W. Weninger), and 632706 (to W. Weninger and J.A. Triccas) and a grant from the NSW government.

The authors have no conflicting financial interests.

Submitted: 1 September 2010

Accepted: 24 January 2011

REFERENCES

- Abadie, V., E. Badell, P. Douillard, D. Ensergueix, P.J.M. Leenen, M. Tanguy, L. Fiette, S. Saeland, B. Gicquel, and N. Winter. 2005. Neutrophils rapidly migrate via lymphatics after *Mycobacterium bovis* BCG intradermal vaccination and shuttle live bacilli to the draining lymph nodes. *Blood*. 106:1843–1850. doi:10.1182/blood-2005-03-1281
- Asarnow, D.M., W.A. Kuziel, M. Bonyhad, R.E. Tigelaar, P.W. Tucker, and J.P. Allison. 1988. Limited diversity of [gamma][delta] antigen receptor genes of thy-1+ dendritic epidermal cells. *Cell*. 55:837–847. doi:10.1016/0092-8674(88)90139-0
- Bergstresser, P.R., R.E. Tigelaar, J.H. Dees, and J.W. Streilein. 1983. Thy-1 antigen-bearing dendritic cells populate murine epidermis. *J. Invest. Dermatol.* 81:286–288. doi:10.1111/1523-1747.ep12518332
- Boismenu, R., and W.L. Havran. 1994. Modulation of epithelial cell growth by intraepithelial gamma delta T cells. *Science*. 266:1253–1255. doi:10.1126/science.7973709
- Bonneville, M., R.L. O'Brien, and W.K. Born. 2010. Gammadelta T cell effector functions: a blend of innate programming and acquired plasticity. *Nat. Rev. Immunol.* 10:467–478. doi:10.1038/nri2781
- Bos, J.D., M.B.M. Teunissen, I. Cairo, S.R. Krieg, M.L. Kapsenberg, P.K. Das, and J. Borst. 1990. T-cell receptor gammadelta bearing cells in normal human skin. *J. Invest. Dermatol.* 94:37–42. doi:10.1111/1523-1747.ep12873333
- Bromley, S.K., S.Y. Thomas, and A.D. Luster. 2005. Chemokine receptor CCR7 guides T cell exit from peripheral tissues and entry into afferent lymphatics. *Nat. Immunol.* 6:895–901. doi:10.1038/ni1240
- Carding, S.R., and P.J. Egan. 2002. [gamma][delta] T cells: functional plasticity and heterogeneity. *Nat. Rev. Immunol.* 2:336–345. doi:10.1038/nri797
- Chinnery, H.R., M.J. Ruitenberg, G.W. Plant, E. Pearlman, S. Jung, and P.G. McMenamin. 2007. The chemokine receptor CX3CR1 mediates homing of MHC class II-Positive cells to the normal mouse corneal epithelium. *Invest. Ophthalmol. Vis. Sci.* 48:1568–1574. doi:10.1167/iovs.06-0746
- Cho, J.S., E.M. Pietras, N.C. Garcia, R.I. Ramos, D.M. Farzam, H.R. Monroe, J.E. Magorien, A. Blauvelt, J.K. Kolls, A.L. Cheung, et al. 2010. IL-17 is essential for host defense against cutaneous *Staphylococcus aureus* infection in mice. *J. Clin. Invest.* 120:1762–1773. doi:10.1172/JCI40891
- Cua, D.J., and C.M. Tato. 2010. Innate IL-17-producing cells: the sentinels of the immune system. *Nat. Rev. Immunol.* 10:479–489. doi:10.1038/nri2800
- De Creus, A., K. Van Beneden, F. Stevenaert, V. Debacker, J. Plum, and G. Leclercq. 2002. Developmental and functional defects of thymic and epidermal v[gamma]3 cells in IL-15-deficient and IFN regulatory factor-1-deficient mice. *J. Immunol.* 168:6486–6493.
- Debes, G.F., C.N. Arnold, A.J. Young, S. Krautwald, M. Lipp, J.B. Hay, and E.C. Butcher. 2005. Chemokine receptor CCR7 required for T lymphocyte exit from peripheral tissues. *Nat. Immunol.* 6:889–894. doi:10.1038/ni1238
- Foster, C.A., H. Yokozeki, K. Rappersberger, F. Koning, B. Volc-Platzer, A. Rieger, J.E. Coligan, K. Wolff, and G. Stingl. 1990. Human epidermal T cells predominantly belong to the lineage expressing α/β T cell receptor. *J. Exp. Med.* 171:997–1013. doi:10.1084/jem.171.4.997
- Girardi, M., D.E. Oppenheim, C.R. Steele, J.M. Lewis, E. Glusac, R. Filler, P. Hobby, B. Sutton, R.E. Tigelaar, and A.C. Hayday. 2001. Regulation of cutaneous malignancy by gamma delta T cells. *Science*. 294:605–609. doi:10.1126/science.1063916
- Girardi, M., J. Lewis, E. Glusac, R.B. Filler, L. Geng, A.C. Hayday, and R.E. Tigelaar. 2002. Resident skin-specific γδ T cells provide local, nonredundant regulation of cutaneous inflammation. *J. Exp. Med.* 195:855–867. doi:10.1084/jem.20012000

- Girardi, M., E. Glusac, R.B. Filler, S.J. Roberts, I. Propperova, J. Lewis, R.E. Tigelaar, and A.C. Hayday. 2003. The distinct contributions of murine T cell receptor (TCR) $\gamma\delta^+$ and TCR $\alpha\beta^+$ T cells to different stages of chemically induced skin cancer. *J. Exp. Med.* 198:747–755. doi:10.1084/jem.20021282
- Glatzel, A., D. Wesch, F. Schiemann, E. Brandt, O. Janssen, and D. Kabelitz. 2002. Patterns of chemokine receptor expression on peripheral blood $\{\gamma\delta\}$ T lymphocytes: strong expression of CCR5 is a selective feature of $\{\gamma\delta\}$ T cells. *J. Immunol.* 168: 4920–4929.
- Havran, W.L., and J.P. Allison. 1988. Developmentally ordered appearance of thymocytes expressing different T-cell antigen receptors. *Nature.* 335:443–445. doi:10.1038/335443a0
- Havran, W.L., S. Grell, G. Duwe, J. Kimura, A. Wilson, A.M. Kruisbeek, R.L. O'Brien, W.K. Born, R.E. Tigelaar, and J.P. Allison. 1989. Limited diversity of T-cell receptor gamma-chain expression of murine Thy-1+ dendritic epidermal cells revealed by V gamma 3-specific monoclonal antibody. *Proc. Natl. Acad. Sci. USA.* 86:4185–4189. doi:10.1073/pnas.86.11.4185
- Havran, W.L., Y.H. Chien, and J.P. Allison. 1991. Recognition of self antigens by skin-derived T cells with invariant gamma delta antigen receptors. *Science.* 252:1430–1432. doi:10.1126/science.1828619
- Hayday, A.C. 2000. $\{\gamma\delta\}$ cells: a right time and a right place for a conserved third way of protection. *Annu. Rev. Immunol.* 18:975–1026. doi:10.1146/annurev.immunol.18.1.975
- Hayday, A.C. 2009. Gammadelta T cells and the lymphoid stress-surveillance response. *Immunity.* 31:184–196.
- Heath, W.R., and E.R. Carbone. 2009. Dendritic cell subsets in primary and secondary T cell responses at body surfaces. *Nat. Immunol.* 10:1237–1244. doi:10.1038/ni.1822
- Heilig, J.S., and S. Tonegawa. 1986. Diversity of murine gamma genes and expression in fetal and adult T lymphocytes. *Nature.* 322:836–840. doi:10.1038/322836a0
- Holtmeier, W., M. Pfänder, A. Hennemann, T.M. Zollner, R. Kaufmann, and W.F. Caspary. 2001. The TCR-delta repertoire in normal human skin is restricted and distinct from the TCR-delta repertoire in the peripheral blood. *J. Invest. Dermatol.* 116:275–280. doi:10.1046/j.1523-1747.2001.01250.x
- Honjo, M., A. Elbe, G. Steiner, I. Assmann, K. Wolff, and G. Stingl. 1990. Thymus-independent generation of Thy-1+ epidermal cells from a pool of Thy-1- bone marrow precursors. *J. Invest. Dermatol.* 95:562–567. doi:10.1111/1523-1747.ep12505543
- Jameson, J., K. Ugarte, N. Chen, P. Yachi, E. Fuchs, R. Boismenu, and W.L. Havran. 2002. A role for skin gammadelta T cells in wound repair. *Science.* 296:747–749. doi:10.1126/science.1069639
- Jensen, K.D., X. Su, S. Shin, L. Li, S. Youssef, S. Yamasaki, L. Steinman, T. Saito, R.M. Locksley, M.M. Davis, et al. 2008. Thymic selection determines gammadelta T cell effector fate: antigen-naïve cells make interleukin-17 and antigen-experienced cells make interferon gamma. *Immunity.* 29:90–100. doi:10.1016/j.immuni.2008.04.022
- Kisielow, J., M. Kopf, and K. Karjalainen. 2008. SCART scavenger receptors identify a novel subset of adult $\gamma\delta$ T cells. *J. Immunol.* 181:1710–1716.
- Kolls, J.K., and A. Lindén. 2004. Interleukin-17 family members and inflammation. *Immunity.* 21:467–476. doi:10.1016/j.immuni.2004.08.018
- Laky, K., L. Lefrançois, U. von Freeden-Jeffry, R. Murray, and L. Puddington. 1998. The role of IL-7 in thymic and extrathymic development of TCR $\{\gamma\delta\}$ cells. *J. Immunol.* 161:707–713.
- Lindén, A., M. Laan, and G.P. Anderson. 2005. Neutrophils, interleukin-17A and lung disease. *Eur. Respir. J.* 25:159–172. doi:10.1183/09031936.04.00032904
- Matheu, M.P., C. Beeton, A. Garcia, V. Chi, S. Rangaraju, O. Safrina, K. Monaghan, M.I. Uemura, D. Li, S. Pal, et al. 2008. Imaging of effector memory T cells during a delayed-type hypersensitivity reaction and suppression by Kv1.3 channel block. *Immunity.* 29:602–614. doi:10.1016/j.immuni.2008.07.015
- Mertsching, E., C. Burdet, and R. Ceredig. 1995. IL-7 transgenic mice: analysis of the role of IL-7 in the differentiation of thymocytes in vivo and in vitro. *Int. Immunol.* 7:401–414. doi:10.1093/intimm/7.3.401
- Miller, M.J., S.H. Wei, I. Parker, and M.D. Cahalan. 2002. Two-photon imaging of lymphocyte motility and antigen response in intact lymph node. *Science.* 296:1869–1873. doi:10.1126/science.1070051
- Moore, T.A., U. von Freeden-Jeffry, R. Murray, and A. Zlotnik. 1996. Inhibition of gamma delta T cell development and early thymocyte maturation in IL-7 $-/-$ mice. *J. Immunol.* 157:2366–2373.
- Mrass, P., H. Takano, L.G. Ng, S. Daxini, M.O. Lasaro, A. Iparraguirre, L.L. Cavanagh, U.H. von Andrian, H.C. Ertl, P.G. Haydon, and W. Weninger. 2006. Random migration precedes stable target cell interactions of tumor-infiltrating T cells. *J. Exp. Med.* 203:2749–2761. doi:10.1084/jem.20060710
- Nakagawa, S., M. Hara, M. Seki, H. Yagita, H. Tagami, and S. Aiba. 1993. Interaction of cutaneous stromal cells and gamma/delta T cell receptor (TcR)-positive cells. I. V gamma 5-gamma/delta TcR+ T cells migrating from organ-cultured murine skin proliferate by co-culture with cutaneous stromal cells in the presence of interleukin-2. *Eur. J. Immunol.* 23:1705–1710. doi:10.1002/eji.1830230746
- Nestle, F.O., P. Di Meglio, J.Z. Qin, and B.J. Nickoloff. 2009. Skin immune sentinels in health and disease. *Nat. Rev. Immunol.* 9:679–691.
- Ng, L.G., A. Hsu, M.A. Mandell, B. Roediger, C. Hoeller, P. Mrass, A. Iparraguirre, L.L. Cavanagh, J.A. Triccas, S.M. Beverley, et al. 2008. Migratory dermal dendritic cells act as rapid sensors of protozoan parasites. *PLoS Pathog.* 4:e1000222. doi:10.1371/journal.ppat.1000222
- Nitahara, A., H. Shimura, A. Ito, K. Tomiyama, M. Ito, and K. Kawai. 2006. NKG2D ligation without T cell receptor engagement triggers both cytotoxicity and cytokine production in dendritic epidermal T cells. *J. Invest. Dermatol.* 126:1052–1058. doi:10.1038/sj.jid.5700112
- Ribot, J.C., A. deBarros, D.J. Pang, J.F. Neves, V. Peperzak, S.J. Roberts, M. Girardi, J. Borst, A.C. Hayday, D.J. Pennington, and B. Silva-Santos. 2009. CD27 is a thymic determinant of the balance between interferon- $\{\gamma\delta\}$ - and interleukin 17-producing $\{\gamma\delta\}$ T cell subsets. *Nat. Immunol.* 10:427–436. doi:10.1038/ni.1717
- Roediger, B., L.G. Ng, A.L. Smith, B.F. de St Groth, and W. Weninger. 2008. Visualizing dendritic cell migration within the skin. *Histochem. Cell Biol.* 130:1131–1146. doi:10.1007/s00418-008-0531-7
- Sharp, L.L., J.M. Jameson, G. Cauvi, and W.L. Havran. 2005. Dendritic epidermal T cells regulate skin homeostasis through local production of insulin-like growth factor 1. *Nat. Immunol.* 6:73–79. doi:10.1038/ni1152
- Shibata, K., H. Yamada, H. Hara, K. Kishihara, and Y. Yoshikai. 2007. Resident Vdelta1+ gammadelta T cells control early infiltration of neutrophils after Escherichia coli infection via IL-17 production. *J. Immunol.* 178: 4466–4472.
- Shibata, K., H. Yamada, R. Nakamura, X. Sun, M. Itsumi, and Y. Yoshikai. 2008. Identification of CD25+ $\{\gamma\delta\}$ T cells as fetal thymus-derived naturally occurring IL-17 producers. *J. Immunol.* 181:5940–5947.
- Tamaki, K., N. Yasaka, C.H. Chang, N. Ohtake, A. Saitoh, K. Nakamura, and M. Furue. 1996. Identification and characterization of novel dermal Thy-1 antigen-bearing dendritic cells in murine skin. *J. Invest. Dermatol.* 106:571–575. doi:10.1111/1523-1747.ep12344049
- Tamura, T., H. Ariga, T. Kinashi, S. Uehara, T. Kikuchi, M. Nakada, T. Tokunaga, W. Xu, A. Kariyone, T. Saito, et al. 2004. The role of antigenic peptide in CD4+ T helper phenotype development in a T cell receptor transgenic model. *Int. Immunol.* 16:1691–1699. doi:10.1093/intimm/dxh170
- Tanaka, Y., C.T. Morita, Y. Tanaka, E. Nieves, M.B. Brenner, and B.R. Bloom. 1995. Natural and synthetic non-peptide antigens recognized by human gamma delta T cells. *Nature.* 375:155–158. doi:10.1038/375155a0
- Triccas, J.A., F.X. Berthet, V. Pelicic, and B. Gicquel. 1999. Use of fluorescence induction and sucrose counterselection to identify *Mycobacterium tuberculosis* genes expressed within host cells. *Microbiology.* 145:2923–2930.
- Tschachler, E., G. Schuler, J. Hutterer, H. Leibl, K. Wolff, and G. Stingl. 1983. Expression of Thy-1 antigen by murine epidermal cells. *J. Invest. Dermatol.* 81:282–285. doi:10.1111/1523-1747.ep12518326
- Ueno, H., N. Schmitt, A.K. Palucka, and J. Banchereau. 2010. Dendritic cells and humoral immunity in humans. *Immunol. Cell Biol.* 88:376–380. doi:10.1038/icb.2010.28
- Unutmaz, D., W. Xiang, M.J. Sunshine, J. Campbell, E. Butcher, and D.R. Littman. 2000. The primate lentiviral receptor Bonzo/STRL33 is coordinately regulated with CCR5 and its expression pattern is conserved between human and mouse. *J. Immunol.* 165:3284–3292.
- Wands, J.M., C.L. Roark, M.K. Aydin, N. Jin, Y. Hahn, L. Cook, X. Yin, J. Dal Porto, M. Lahn, D.M. Hyde, et al. 2005. Distribution and leukocyte

- contacts of $\gamma\delta$ T cells in the lung. *J. Leukoc. Biol.* 78:1086–1096. doi:10.1189/jlb.0505244
- Williams, I.R., E.A. Rawson, L. Manning, T. Karaoli, B.E. Rich, and T.S. Kupper. 1997. IL-7 overexpression in transgenic mouse keratinocytes causes a lymphoproliferative skin disease dominated by intermediate TCR cells: evidence for a hierarchy in IL-7 responsiveness among cutaneous T cells. *J. Immunol.* 159:3044–3056.
- Xiong, N., and D.H. Raulet. 2007. Development and selection of gamma delta T cells. *Immunol. Rev.* 215:15–31. doi:10.1111/j.1600-065X.2006.00478.x
- Yoshida, R., M. Nagira, M. Kitauro, N. Imagawa, T. Imai, and O. Yoshie. 1998. Secondary lymphoid-tissue chemokine is a functional ligand for the CC chemokine receptor CCR7. *J. Biol. Chem.* 273:7118–7122. doi:10.1074/jbc.273.12.7118